In-Situ Assessment of PEM Fuel Cells via AC Impedance at Operational Loads

Wenhua H. Zhu, Robert U. Payne, Donald R. Cahela, and Bruce J. Tatarchuk*
Center for Microfibrous Materials Manufacturing
Department of Chemical Engineering
230 Ross Hall, Auburn University, AL 36849

Abstract   PEM fuel cells in a Ballard Nexa[TM] stack were analyzed via AC impedance using a Gamry FC350[TM] monitor and a TDI electronic load. Single MEAs, multiple MEA cell groups, and full 47 MEA stacks were examined. Impedance results were successfully fit to equivalent circuit diagrams containing charge transfer polarization resistances related to activation energies, uncompensated resistances related to the electrolytes, and double layer capacitances related to the surface area of the electrocatalysts. AC impedance was successfully conducted on the fuel cell stack at over 46 A stack currents (~383.3 mA/cm^2). From AC impedance data collected at different currents, the rate limiting behavior of various components and physical processes are determined. Good agreement is obtained between the circuit elements and physical processes determined via AC impedance and independent measurements of these same elements by other means. AC impedance appears to be a simple and easy method to implement in-situ real time diagnostic capability suitable for assessing the behavior and state-of-health of the PEM stack.

Keywords: AC impedance; proton exchange membrane fuel cells; fuel cell stack; system diagnosis.

The commercial PEM fuel cell products exhibit a wide range of choices but their performance may rapidly deteriorate due to unprofessional usage. The real time performance and behavior for the fuel cell(s) in the operational system have some difference in comparison with simple tests of single cell or multiple cell groups—stack. It is important to identify a product for certain applications such as low-high power densities, long life operation,

 * Corresponding author. Tel.: +1-334-844-2023; E-mail address: brucet@eng.auburn.edu.

or peak pulse requirement. Authors (Springer *et al*., 1995 and 1999) reported PEM fuel cell work by using electrochemical impedance spectroscopy (EIS), which describes the response of a circuit to an alternating current or voltage as a function of frequency. Impedance data analysis is capable of determining the fuel cell power losses from ohmic, kinetic, and mass transport data. The advantage is that the EIS technique can use a purely electronic model (equivalent circuit diagram) to represent an electrochemical fuel cell. Further, accurate data simulation and interpretation insures that the equivalent circuit model describes the real physical phenomena in the PEM fuel cell system more precisely. The purpose of the work described in the present paper is to operate the commercial PEM fuel cells at different load levels and obtain the real time impedance data for the PEM fuel system.

The commercial fuel cell systems of the Nexa[TM] Power Module (Ballard Power Systems) were taken to the lab for EIS test. The traditional EG&G AC impedance system (Model Potentiostat/galvanostat 273A and Model 5210 Lock-in amplifier) was usually limited to about 1 A and 10 V. Although the Ballard Nexa[TM] fuel cell system is a small fuel cell system providing 1200 watts of unregulated DC power at a nominal output voltage of 26 VDC, its output current can reach 44 A and voltage usually up to 42 V. The Nexa[TM] system has a central controller, air compressor and other electrical devices which consume electric power from the fuel cell stack, making the accurate EIS measurement more difficult. Another Nexa[TM] system was started up and provided a similar power source to control the system electronic devices. The stack was successfully decoupled from the system for EIS measurement. The stack power exchange was
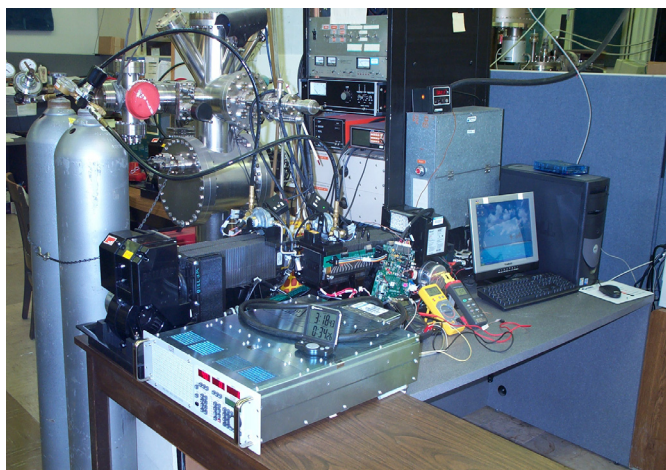
Figure 1. AC impedance test equipment for Ballard Nexa[TM] system.

only conducted at the EIS testing stage and the fuel cell system still proceeded with its original startup and shutdown process for safety reasons. Gamry FC350[TM] fuel cell monitor with a TDI electric load is capable of measuring the impedance of operating fuel cells at high current levels (Gamry Instruments, Warminster, PA). The fuel cell monitor uses the electric load to sink the fuel cell current.

The experimental arrangement of the FC350, the TDI electronic load and the fuel cell system are shown in Figure 1. The sinusoidal current signal from the FC350, working in galvanostatic impedance mode, modulates the current from single or multiple fuel cell(s) or the FC stack. The current information at the electric load is sent to the FC350[TM] monitor at the same time. The fuel cell voltage is measured by the FC350 directly. The FC350 collects these data and generates the impedance. The small excitation waveforms of this amplitude caused only minimal perturbation of the FC system and reduced errors caused by the measurement technique. The level of noise in the impedance data depends on the size of current and voltage signals returned to the frequency response analyzer. The Gamry Hybrid EIS mode was applied for the experiments in order to observe the EIS behavior at low frequencies. The use of the Gamry FC350 monitor and TDI electronic load can obtain better results on ultra-low impedance analysis at a high power output.

After the Nexa[TM] system was operated

to a steady state at a certain level of power output through the TDI electronic load, the control system and all other electronic devices were switched to external power from another Nexa[TM] system without power interruption. The Nexa[TM] #308 was first tested by applying a 20 mV AC voltage, *i.e.* Hybrid EIS technique. The system used constant current operation before applying the 20 mV AC signal. For the whole stack test, the Bode plots and Nyquist curves are shown in Figure 2 and Figure 5. At a frequency of more than 10 Hz, the real part of the impedance is less than 0.215 Ω and the plots at 3 current levels are overlapped in Figure 2. For the 47th single cell test, the semicircle loop is followed by an additional finite diffusion at the low frequency side of the Nyquist plots (Figure 3), but has not happened in the single cell test from the 10th cell to 42nd cell. This means that mass transport is limiting the stack performance. The resistance related to mass transport is caused by gas diffusion or water flooding and may result mainly from inert gas buildup at lower power output. Periodical purge at the anode side is necessary to remove the anode side polarization. This phenomenon is also noticed in the test of multiple cell groups. The Nyquist plots of the multiple cell tests are shown in Figure 4. The test on the 1st-47th cell group including the 47th cell (at end of stack, *i.e.*, the hydrogen outlet side) also shows an additional finite diffusion following the semicircle loop at the low frequency side of in the Nyquist plots. Impedance data
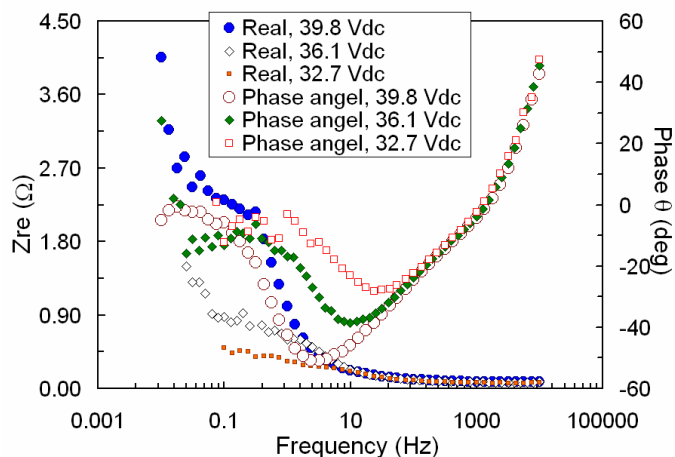

Figure 2. Bode plots of Nexa[TM] #308 PEM fuel cell stack. Air 2.2 psig, H$_2$ 5.0 psig, working area ~120 cm^2 for each fuel cell.
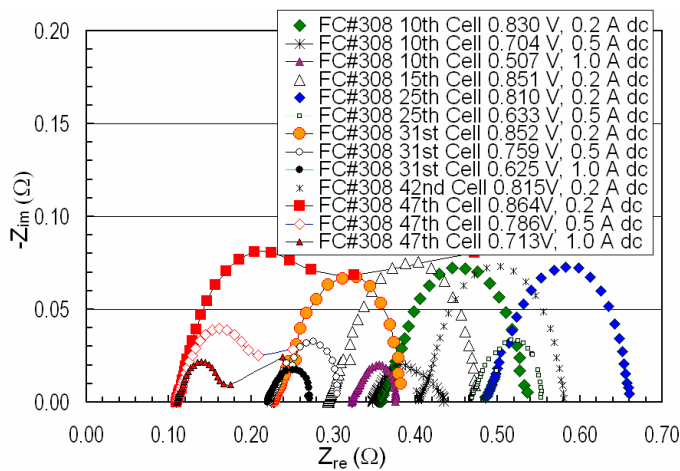
Figure 3. Nyquist plots of single fuel cell in Nexa™ #308 PEM stack. Air 2.2 psig, H_2 5.0 psig, working area ~120 cm^2.

Figure 4. Nyquist plots of multiple fuel cell group in the Nexa™ #308 PEM stack. Air 2.2 psig, H_2 5.0 psig, working area ~120 cm^2.

reveal that the exhaust management of a few cells at the end of the stack is important to the system performance, because mass transport limitation occurs at the end section of the stack. The exhaust purge and higher flow rate at the outlet side of the anode is essential to remove the inert polarization in the gas diffusion electrodes.

Further impedance test on the Nexa™ stack are shown in Fig. 5 and Fig. 6. Figure 6 is the magnified result from Figure 5, for clarity at higher current output. The polarization resistance (diameter R_p) at low frequencies decreases rapidly with an increase in operating current. The data at lower frequencies is noisier than at high frequencies. This noise at a high operating current reveals that one or more limitations occur inside the gas diffusion electrodes or the fuel cell system. The main reason is considered to be mass transport limitation resulting from the accumulation of inert gases or product water flooding/evaporating inside the gas diffusion electrodes. The up-tails of the semicircle indicate that mass transport by diffusion of air (oxygen consumption and nitrogen exhaust), water (gas and liquid removal), and fuel gas (hydrogen oxidation and inert accumulation) limit the fuel cell performance because of high demands on fuel/oxidant and product removal at high current densities. From the above tests, it is also concluded that mass transport limitation occurs in the anodes of a
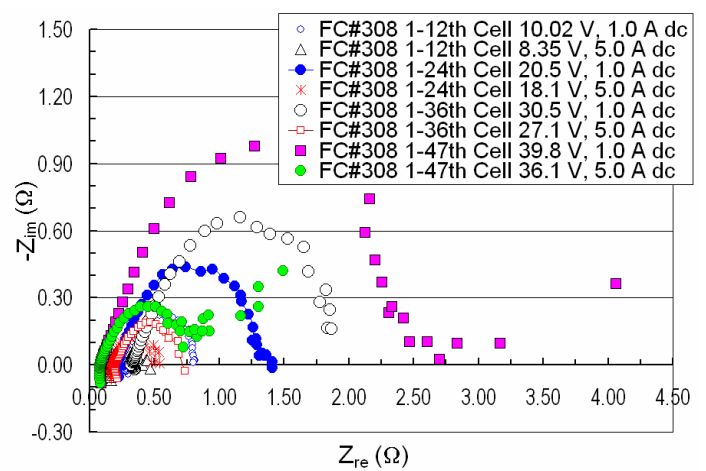
few fuel cells at the end of the hydrogen outlet side at lower current densities.

Impedance tests were performed on the fuel cell stack with system controller and electronic devices at different current levels (Figure 7). The parameters shown in the graph are stack voltage/current before testing and applied AC signals for impedance tests. The impedance results are noisier than the data in Figure 5, mainly due to the control system and electronic devices. From the comparison of these test data at the same current level, the difference resulting from the switches and electronic devices is capable of being identified. Detailed in-situ tests of separation and comparison of the fuel cell stack and system
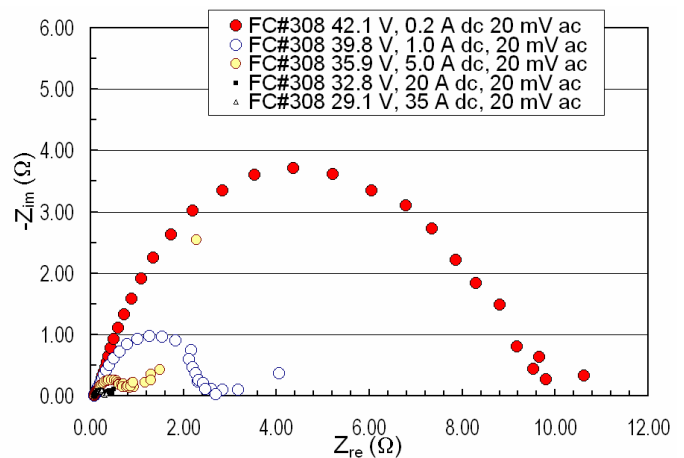

Figure 5. Nyquist plots of Nexa™ #308 PEM fuel cell stack. Air 2.2 psig, H_2 5.0 psig, working area ~120 cm^2.
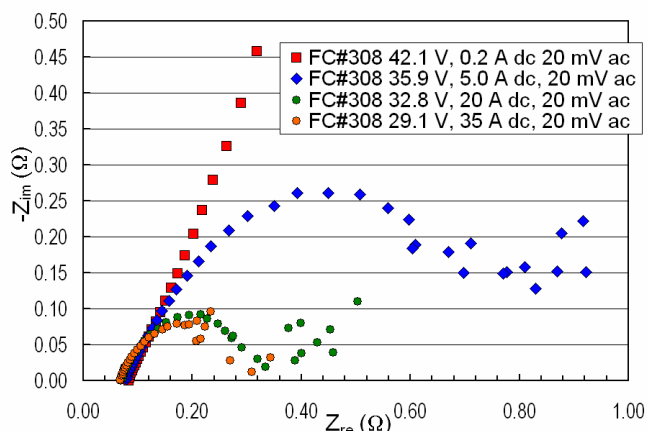
Figure 6. Detailed Nyquist plots of Nexa[TM] #308 fuel cell stack at higher power output levels. Air 2.2 psig, H_2 5.0 psig, working area ~120 cm^2.

are in further development and potentially beneficial for system analysis and design.

The in-situ impedance data using NLLS fitting were quantitatively analyzed in order to estimate the ohmic, kinetic resistance and double layer capacitance. The physical parameters were simulated and applied to generate the equivalent circuit diagram. The cell impedance at more than 10 kHz frequency is corresponds to the membrane resistance. In general, the anode impedance can be neglected in the low frequency range (Wagner, 2002) because the impedance is mainly contributed by
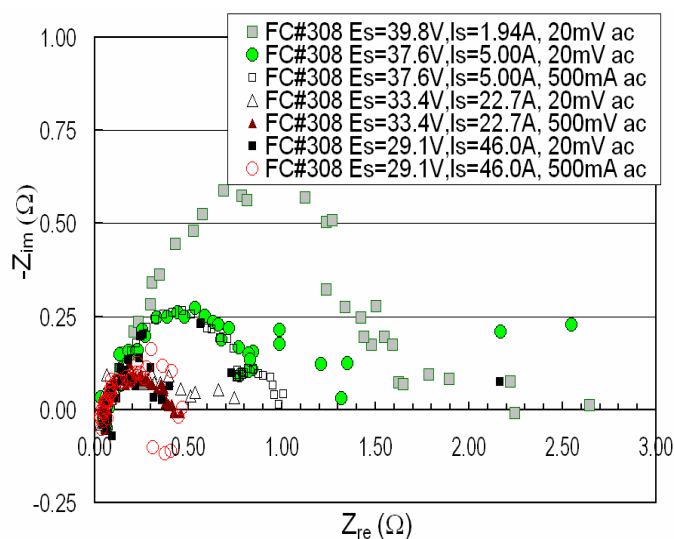

Figure 7. Nyquist plots of Nexa[TM] #308 fuel cell stack with electronic devices. Air 2.2 psig, H_2 5.0 psig, stack voltage/current before impedance test and applied ac listed in the legend.

the cathodes and membranes at normal operating conditions. The other impedance can be attributed to the bipolar plates, current collectors, wires plus contact impedance, and anode inert polarization in stacks. The average contact and wire resistance is estimated as 28 mΩ through voltage drop at a certain current. The electrolyte resistance between the cathode and the anode must be considered when modeling the cell or stack. The resistance of protons in the polymer membrane electrolyte (R_m) depends on its concentration, membrane type, temperature and the geometry of the area in which current is carried. The uncompensated resistance R_Ω slightly decreases when increasing current in the circuit because of cell temperature and membrane humidity increase. The diameter of the semicircle in Nyquist diagrams is the polarization resistance (R_{ct}, *i.e.* related to the charge transfer resistance). It is related to the kinetics of the reactions and the diffusion of the reactants both towards and away from the electrodes. The R_{ct} reduces rapidly as applied current and temperature increase. Lower R_{ct} values at high current (35 A) and high temperature (67°C) reveal that the fuel cells are well activated and available for higher power output. The uncompensated resistance R_Ω at 35 A stack current (47 cells in series) is 0.0736 Ω (~188 mΩ-cm^2), which approximately matches the membrane electrolyte resistance of *ca.* 0.18 Ω-cm^2 (Ciureanu and Roberge *et al.*, 2001). There is an electrical double layer existing at the interface between an electrode and its electrolyte. The double layer capacitance drops off at *ca.* 0.0386 F when output current increases from 0.2 A to 5 A. At higher currents, the double layer capacitance exhibits only a small change when the system is loaded from 5 A to 35 A. This capacitance prospectively improves the system's pulse capability through loading of a proper catalyst. The system was further tested in 46 A (~383.3 mA/cm^2) and 1339 W stack power with the system controller. The uncompensated resistance at 46 A stack current (47 cells in series) is approximately 0.050 Ω. This data is very close to the R_Ω value of 0.056 Ω when tested at 22.7 A and 758 W with the same op-

erating temperature level. The in-situ assessment of PEM fuel cells and stack in the Nexa[TM] system was performed via AC Impedance at operational loads. The impedance data for single fuel cells, multiple cell groups, and the fuel cell stack in the real system were obtained and analyzed. With the system controller, the uncompensated resistance R_Ω at 46 A stack current (47 cells in series, ~383.3 mA/cm^2) is approximately 0.050 Ω (127.7 mΩ-cm^2). From AC impedance data collected at different currents, the rate limiting behavior of various components and physical processes are also determined by separation of the electronic devices from the fuel cell system. Good agreement is obtained between the circuit elements and physical processes determined via AC impedance and independent measurements of these same elements by other means. For the fuel cell(s) and its stack with the separated controller and electronic devices, AC impedance in-situ measurement, data analysis is developed to be a potential valid method to implement the real time evaluation of the PEM fuel cell(s) and its stack for its real time power capability and lifetime for further operation.

Acknowledgements

References

Ciureanu, M. and Roberge, R., J. Phys. Chem., B105, 3531-3539 (2001).

Springer, T. E., Proceedings of Electrochem. Soc., 99-14, pp.208-221, 1999.

Springer, T. E., Zawodzinski, T. A., Wilson, M. S., and Gottesfeld, S., Proceedings of Electrochem. Soc., 95-23, pp.137-151, 1995.

Wagner, N., J. Applied Electrochemistry, 32, 859-863 (2002).